

High-Throughput Computational Search for Two-Dimensional Binary Alloys: Energetic Stability versus Synthesizability of Three-Dimensional Counterparts

Shota Ono* and Honoka Satomi

Department of Electrical, Electronic and Computer Engineering, Gifu University, Gifu 501-1193, Japan

Using first principles calculations, the energetic stability of two-dimensional (2D) binary alloys XY is investigated, where X and Y indicate the metallic element from Li to Pb in the periodic table, i.e., the total number of 1081 alloys. The formation energy of 2D alloys in the buckled honeycomb (bHC) lattice structure is correlated to that of three-dimensional alloys in the B_h structure. By performing phonon dispersion calculations, we show that if an alloy in the B_h structure has been synthesized experimentally, that in the bHC structure is dynamically stable. In contrast, an alloy in the bHC structure is unstable, that in the B_h structure has not been synthesized yet. The negatively large formation energy is not a necessary and sufficient condition for yielding the dynamical stability of alloys.

Introduction. Recent advances have expanded the family of two-dimensional (2D) materials including graphene, black phosphorene, and transition metal dichalcogenides, and so forth, which can have a strong impact on scientific and technological innovation due to their electronic, mechanical, and optical properties [1]. Despite its growing members in the 2D materials, design principles for creating 2D materials have not been established. Intuitively, the structure of stable 2D materials is a counterpart of stable three-dimensional (3D) materials. For example, silicene is atomically thin layer of silicon atoms constructed from the (111) surface of silicon diamond structure [2]. The validity of this concept has been confirmed in 2D metals including gallene (Ga) [3], bismuthene (Bi) [4], poloniumene (Po) [5], and most elements in the periodic table [6–8]: For noble metals, the monolayer hexagonal and buckled honeycomb (bHC) structures are dynamically stable, as they can be constructed from the (111) surface of the fcc and/or hcp structures. However, it remains unclear whether this rule can be applied to alloys, where many crystal structures exist depending on the constituents of alloys, temperatures, and pressures. Recently, it has been reported that CuAu alloy can have a 2D structure, where hexagonal layers of Cu and Au are stacked to form a bilayer structure [9], while CuAu has been known to have $L1_0$ structure.

As the computational capacity is increasing with time, high-throughput (HT) density-functional theory (DFT) methods enables us to carry out materials design [10]. For example, it has been applied to identify new phases of binary alloys based on platinum-group metals [11] and high-entropy alloys [12]. Recent HT-DFT studies have proposed various criteria that identify the stability of 2D materials. For example, the exfoliation energy of 2D layers [13] and the relative difference between experimental lattice constants and DFT based lattice constants [14] are used to predict possible 2D materials.

In this Letter, by using HT-DFT, we search for 2D binary alloys that are energetically and dynamically stable.

We focus on the ordered structures only. First, we investigate the energetic stability of 1081 binary alloys, created from the combination of 46 metallic elements, in the bHC and buckled square (bSQ) structures (see Fig. 1). These buckled structures for alloys are natural extensions of those for simple metals [7, 8], and the former bHC has been realized in 2D CuAu [9]. For comparison, $L1_0$, B_h , and B2 structures are also studied, which correspond to the fcc, hcp, and bcc structures in simple metals, respectively. We demonstrate that a strong correlation of the formation energy between bHC and B_h structures is present. We then extract 40 candidates for 2D alloys with the help of Material Informatics database. By performing phonon dispersion calculations, we demonstrate that four alloys in the bHC structure, as analog of 3D alloys in the B_h structure, are dynamically stable. In contrast, 11 alloys in the bHC structure is unstable because those in the B_h structure have not been synthesized yet.

One of the open questions in materials science is to predict which structures can be created experimentally, i.e., *the synthesizability*. In general, the presence of metastable structures created experimentally can be rationalized by not the energetic stability only but the overall structure of potential energy surface, characterized by many degrees of freedom (i.e., the atom positions) [15–17]. For example, high energy barriers are necessary for preventing the metastable structure from transforming into more stable structures against perturbations [15]. As an approach beyond the formation energy analysis, we focus on the synthesizability of B_h structure and relate it to the dynamical stability of 2D structure in binary alloys. Our approach can serve as an alternative method for materials design in computational materials science, leading to novel materials synthesis.

Computational details. We calculate the total energy of alloys based on DFT implemented in **Quantum ESPRESSO (QE)** code [18]. The effects of exchange and correlation are treated within GGA-PBE [19]. We use the ultrasoft pseudopotentials generated by the scheme of Ref. [20], i.e., **pslibrary.1.0.0**. The cutoff ener-

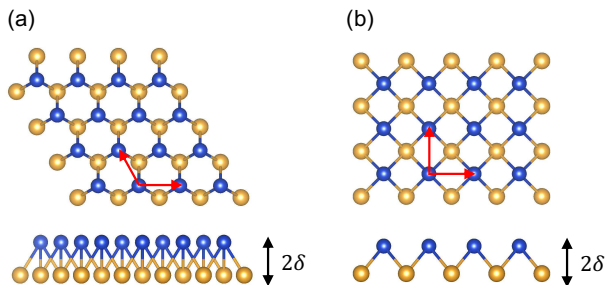


FIG. 1: Schematic illustration for binary alloys in the (a) bHC and (b) bSQ structures. The buckling height is expressed by δ (total thickness 2δ). The primitive lattice vectors are indicated by arrows (red).

gies for the wavefunction and the charge density are 80 and 800 Ry, respectively. The self-consistent calculations within spin-restricted approximation are performed by using $20 \times 20 \times 1$ k grid and $20 \times 20 \times 20$ k grid for 2D and 3D structures, respectively [21]. The smearing parameter of Marzari-Vanderbilt [22] is set to $\sigma = 0.02$ Ry. For 2D structures, we set the size of the unit cell along the c axis to be 14 Å that is enough to avoid the interlayer coupling between different unit cells. The total energy and forces are converged within 10^{-4} Ry and 10^{-3} a.u., respectively.

We define the formation energy of the binary alloy XY in the structure j as

$$E_j(XY) = \varepsilon_j(XY) - \frac{1}{2} [\varepsilon_j(XX) + \varepsilon_j(YY)], \quad (1)$$

where the values of $\varepsilon_j(XY)$ is the total energy of alloy XY in the structure j that is either bHC, bSQ, $L1_0$, B_h , or B2 in the present work. Negative value of $E_j(XY)$ indicates that alloying yields energetically more stable structure.

We first optimize the lattice constant a of the binary alloy XY in the B2 structure. For the geometry optimization of the other structures, the initial guess for a is set to be the value of a optimized for B2 structure. For bHC and bSQ, the buckling height δ is assumed to be $0.3a$ (total thickness 2δ). For computational efficiency, we will not study which the high and low buckled structures are more stable, unless noted otherwise, and will focus on the trend of the stability of 2D alloys only. For the $L1_0$ structure, the initial guess for c/a is set to be 1.1 and 0.9. The lower energy structure is assigned to be $L1_0$ below. For the B_h structure, the initial guess of c/a is set to be the ideal value of 1.63. For a few alloys except in the B2 structure, the self-consistent field calculations have failed to converge: AuCs, BaPt, CsCu, CsPd, and CuRb in the bHC structure, CaPt, CsCu, CuK, and CuRb in the bSQ structure, CsCu in the $L1_0$ structure, and BaPt, BeNa, CsCu, and CuRb in the B_h structure. This implies that no ordered phase is present for these alloys.

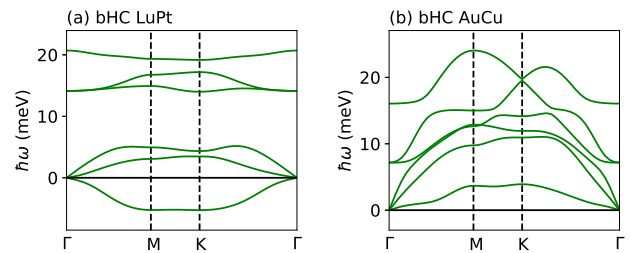


FIG. 2: The phonon dispersion curves of (a) LuPt and (b) AuCu in the bHC structure.

The phonon dispersion calculations are performed within the density-functional perturbation theory [23] implemented in QE code [18] and by using more than $6 \times 6 \times 1$ q grid, that is, 7 q points for bHC and 10 q points for bSQ structures. When small imaginary frequencies are present around Γ point for bHC structure, $8 \times 8 \times 1$ q grid (10 q points) is used (the cases of LiMg, LiRh, and MoRh), which can lead to positive values of frequencies around Γ . In the present study, imaginary frequency of ω is represented by negative value.

Energetic stability and dynamical stability. We have found 220 bHC and 324 bSQ alloys having negative formation energy. Among bHC alloys, LuPt has the lowest formation energy, that is, $E_{\text{bHC}}(\text{LuPt}) = -1.35$ eV. Motivated by this fact, we investigate the dynamical stability of bHC LuPt. The phonon dispersion curves along the symmetry lines are shown in Fig. 2(a). The bHC LuPt is unstable because imaginary frequencies are observed around points M and K, irrespective to the lowest $E_{\text{bHC}}(XY)$. Similarly, bSQ LuPt that has the lowest $E_{\text{bSQ}}(XY)$ is dynamically unstable.

Next, we focus on bHC AuCu. Although $E_{\text{bHC}}(\text{AuCu})$ has a positive value (0.22 eV), bHC AuCu is dynamically stable as shown in Fig. 2(b). This supports the recent experiment [9], where bHC AuCu is synthesized on graphene substrate. Note that the use of GGA-PBE functional [19] to AuCu is known to yield an underestimation of the formation energy of ordered phases ($L1_0$ and $L1_2$) by a factor of two. While the use of nonlocal functional is necessary to predict the value of the formation energy correctly [24], we believe that more accurate calculations also produce the dynamical stability of bHC AuCu. In addition, the value of E_{bHC} as well as the dynamical stability may depend on the substrate, while such investigations are beyond the scope of this work.

Through the phonon dispersion calculations on bHC LuPt and AuCu, we point out that negatively large formation energy of the structure j is not a necessary and sufficient condition for obtaining dynamically stable alloys in the structure j . Similar stability properties have been reported in silicene and germanene [2] and 2D simple metals [8].

Synthesizability and dynamical stability. Although the

TABLE I: List of alloys that satisfy the conditions (i) and (ii) described in text. “SE” and “NR” indicate that B_h structure has been “synthesized experimentally” and has “not been reported”, respectively. “DS” and “U” indicate that bHC structure is “dynamically stable” and “unstable”, respectively. The figure in the parenthesis is the number of alloys that match the conditions imposed.

B_h SE / bHC DS	: IrLi, LiPd, LiPt, and LiRh (4)
B_h SE / bHC U	(0)
B_h NR / bHC DS	: AgAl, AgAu, AgPd, AgPt, AuCd, CdMg, CrIr, CrRh, FeGa, GaMg, IrMo, IrRe, IrRu, IrTc, IrW IrZn, LiMg, MgSn, MoRh, OsRe, OsRu, ReTc, RhTc, RuTc, and ScZr (25)
B_h NR / bHC U	: AgZn, AlTi, AuTi, CaZn, GaTc, GaV, MgZn, MoPt, OsV, PtRe, and PtTc (11)

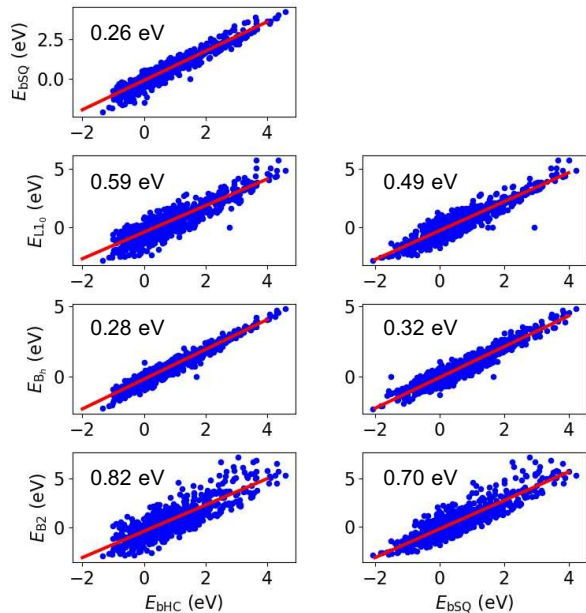


FIG. 3: The relationship of $E_j(XY)$ between different structures. The least mean square fit is indicated by the straight line (red). The standard deviation from the fit is also indicated.

size of $E_j(XY)$ may not be an important factor in predicting the dynamical stability of metastable structures, it would be useful to investigate a similarity of alloys in between different structures [6]. Figure 3 show the relationship of $E_j(XY)$ between the bHC, bSQ, L1₀, B_h , and B2 structures. The least square fit is indicated by straight line. The size of $E_{bHC}(XY)$ and $E_{bSQ}(XY)$ is well correlated to that of 3D structures. In particular, a strong correlation between the bHC and B_h structures is observed: The standard deviation from the least square fit is 0.28 eV. This must reflect the fact that both bHC and B_h structures can be constructed by stacking the hexagonal lattice, and would influence the relationship of dynamical stability between the bHC and B_h structures.

In order to study the metastability of B_h alloys in the bHC structure, we choose binary alloys that can have

B_h structure (space group of $P\bar{6}m2$), negative formation energy, and zero band gap, referring to Materials Project database [25] and using pymatgen code [26]. We find that 40 alloys satisfy these conditions and identify that among them 29 alloys are dynamically stable. Table I lists the number of alloys satisfying the conditions: (i) the B_h structure has been synthesized experimentally and (ii) the bHC structure is dynamically stable. The Li-based alloys of IrLi, LiPd, LiPt, and LiRh satisfy both conditions. No alloys are found for satisfying the condition (i) only. Therefore, this establishes the structure-stability relationship: If a binary alloy in the B_h structure has been synthesized experimentally, that in the bHC structure is dynamically stable ($B_h \rightarrow$ bHC). We have also found that 11 alloys are unstable (see Table I), and quite interestingly, those in the B_h structure have not been synthesized experimentally [25]. Therefore, the contraposition of “ $B_h \rightarrow$ bHC” also holds. The phonon dispersions of these alloys in the bHC structure are provided in Supplemental Materials (SM) [27].

We can confirm that the negatively large formation energy is not a necessary and sufficient condition for the dynamical stability of alloys, again. The values of E_{bHC} for the stable Li-based alloys are as follows: For IrLi, LiPd, LiPt, and LiRh, $E_{bHC} = -0.47, -0.70, -1.02,$ and -0.28 eV, respectively. On the other hand, the values of E_{bHC} for most of unstable alloys are larger than zero, whereas $E_{bHC}(\text{MoPt}) = -0.64$ and $E_{bHC}(\text{OsV}) = -0.27$ eV, which are comparable to the Li-based alloys. bHC FeGa has the most largest value of $E_{bHC} = 0.58$ eV, irrespective to its dynamical stability.

The relationship of $B_h \rightarrow$ bHC is not due to the Li-mediated stabilization. To prove it, we investigate the dynamical stability of 45 Li-based alloys in the bHC structure by calculating phonon dispersions. We have confirmed that most of Li-based alloys in the bHC structure are unstable except AgLi, AlLi, AuLi, CoLi, CuLi, GaLi, IrLi, LiLu, LiMg, LiNi, LiPd, LiPt, LiRh, LiSc, LiY, LiTl, and LiY (bHC Li is also stable [8]).

When the condition of negative formation energy is not imposed in the search of B_h alloys [26], we find 96 alloys that consist of metallic elements only. AlSn alloy has already been synthesized experimentally only, in addition

to the Li-based alloys mentioned above [25]. Thus, we investigate the dynamical stability of AlSn by considering three different bHC structures: no buckled, low-buckled, and high-buckled structures. Unfortunately, all structures are unstable. This may be due to the instability of AlSn in the B_h structure within GGA-PBE level. The phonon dispersion curves in these structures are shown in SM [27]. Even when the PBEsol functional [28] is used, AlSn alloys in the B_h and bHC structures are unstable. It is desired to use nonlocal potentials such as described in [24] for studying the dynamical stability of AlSn alloys.

The present investigation implies that there would be two scenarios for the dynamical stability of alloys in the bHC structure. One is explained as a 2D analog of the B_h structure that has been already synthesized (that is, the hexagonal symmetry is preferred), which supports the stability of four Li-based alloys listed in Table I. The other might be more complex: although the ground state structure is different from the B_h structure, a few or more metastable structures that can be correlated with the bHC structure, as in Fig. 3, are hidden in the potential energy surface, which can yield dynamically stable alloys in the bHC structure. While this is still a phenomenological discussion, we believe that the latter scenario explains the stability of the other 25 alloys (see Table I) and $L1_0$ AuCu [9]. In the previous study [8], we have demonstrated that AlCu in the B_h structure is dynamically stable due to the similarity of the stability properties between Al and Cu layers, while such a structure has not been synthesized yet. We include AlCu alloy to the latter group because that in the bHC structure is found to be dynamically stable (see SM [27] for the phonon dispersions).

It would be helpful to note that when bSQ structure is assumed, 10 alloys of AlTi, IrRe, IrRu, IrTc, LiMg, OsRe, OsRu, ReTc, RuTc, and ScZr are found to be dynamically stable. These alloys in the B_h structure have not been synthesized yet. In addition, most of these may have no ordered phase [25]. It is interesting to note that PbSn₃ and BiSn₃ monolayers have been synthesized on Rh(111) surface [29, 30], although in Pb-Sn and Bi-Sn alloys no 3D ordered structures have been synthesized experimentally [25]. In this sense, we expect that most of alloys in the bHC and bSQ structures proposed in this study can be created by using appropriate substrates.

Conclusion and future prospects. We have demonstrated that negatively large formation energy is not a necessary and sufficient condition for yielding dynamically stable alloys, as in LuPt and AuCu. By systematically calculating the formation energy of ordered alloys, we have shown that a strong correlation is present in between bHC and B_h structures. We have proposed the relationship between the synthesizability of B_h alloys and the dynamical stability of those in the bHC structure. We have identified 29 binary alloys as candidates having the bHC structure.

The present strategy for finding 2D alloys, relating the different structures in different dimensions, can be extended to other 2D structures. For example, the instability of bHC LuPt (see Fig. 2(a)) is due to the different ground state structure in the 3D crystal: Lu and Pt form the $L1_2$ structure. We consider that as a counterpart of $L1_2$, other 2D structures must be present. In this respect, the origin of the dynamical stability of 25 alloys listed in Table I as well as $L1_0$ AuCu, shown in Fig. 2(b) and reported in Ref. [9], remains unclear. In the present investigation, we have focused on alloys that consist of metallic elements only. We expect that the stability relationship between B_h and bHC structures can also be applied to other B_h compounds that include other elements such as C, N, and S (230 alloys [26]) and that more analyses, with the help of 2D materials database [13, 14, 31], can lead to an establishment of another stability-synthesizability relationship.

The authors thank M. Aoki for fruitful discussions. The computation was carried out using the facilities of the Supercomputer Center, the Institute for Solid State Physics, the University of Tokyo, and using the supercomputer “Flow” at Information Technology Center, Nagoya University.

* Electronic address: shota_o@gifu-u.ac.jp

- [1] P. Ajayan, P. Kim, and K. Banerjee, Two-dimensional van der Waals materials, *Phys. Today* **69**(9), 38 (2016).
- [2] S. Cahangirov, M. Topsakal, E. Aktürk, H. Şahin, and S. Ciraci, Two- and One-Dimensional Honeycomb Structures of Silicon and Germanium, *Phys. Rev. Lett.* **102**, 236804 (2009).
- [3] V. Kochat, A. Samanta, Y. Zhang, S. Bhowmick, P. Manimunda, S. A. S. Asif, A. S. Stender, R. Vajtai, A. K. Singh, C. S. Tiwary, P. M. Ajayan, Atomically thin gallium layers from solid-melt exfoliation. *Sci. Adv.* **4**, e1701373 (2018).
- [4] E. Aktürk, O. Ü. Aktürk, and S. Ciraci, Single and bilayer bismuthene: Stability at high temperature and mechanical and electronic properties, *Phys. Rev. B* **94**, 014115 (2016).
- [5] S. Ono, Two-dimensional square lattice polonium stabilized by the spin-orbit coupling, *Sci. Rep.* **10**, 11810 (2020).
- [6] J. Nevalaita and P. Koskinen, Atlas for the properties of elemental two-dimensional metals, *Phys. Rev. B* **97**, 035411 (2018).
- [7] J. Hwang, Y. J. Oh, J. Kim, M. M. Sung, and K. Cho, Atomically thin transition metal layers: Atomic layer stabilization and metal-semiconductor transition, *J. Appl. Phys.* **123**, 154301 (2018).
- [8] S. Ono, Dynamical stability of two-dimensional metals in the periodic table, *Phys. Rev. B* **102**, 165424 (2020).
- [9] G. Zagler, M. Reticcioli, C. Mangler, D. Scheinecker, C. Franchini, and J. Kotakoski, CuAu, a hexagonal two-dimensional metal, *2D Mater.* **7**, 045017 (2020).
- [10] G. R. Schleder, A. C. M. Padilha, C. M. Acosta, M.

- Costa, and A. Fazzio, From DFT to machine learning: recent approaches to materials science—a review, *J. Phys.: Mater.* **2**, 032001 (2019).
- [11] G. L. W. Hart, S. Curtarolo, T. B. Massalski, and O. Levy, Comprehensive Search for New Phases and Compounds in Binary Alloy Systems Based on Platinum-Group Metals, Using a Computational First-Principles Approach, *Phys. Rev. X* **3**, 041035 (2013).
- [12] M. C. Tropicovsky, J. R. Morris, P. R. C. Kent, A. R. Lupini, and G. M. Stocks, Criteria for Predicting the Formation of Single-Phase High-Entropy Alloys, *Phys. Rev. X* **5**, 011041 (2015).
- [13] M. Ashton, J. Paul, S. B. Sinnott, and R. G. Hennig, Topology-Scaling Identification of Layered Solids and Stable Exfoliated 2D Materials, *Phys. Rev. Lett.* **118**, 106101 (2017).
- [14] K. Choudhary, I. Kalish, R. Beams, and F. Tavazza, High-throughput Identification and Characterization of Two-dimensional Materials using Density functional theory, *Sci. Rep.* **7**, 5179 (2017).
- [15] C. P. Ewels, X. Rocquefelte, H. W. Kroto, M. J. Rayson, P. R. Briddon, and M. I. Heggie, Predicting experimentally stable allotropes: Instability of penta-graphene, *PNAS* **112**, 15609 (2015).
- [16] W. Sun, S. T. Dacek, S. P. Ong, G. Hautier, A. Jain, W. D. Richards, A. C. Gamst, K. A. Persson, G. Ceder, The thermodynamic scale of inorganic crystalline metastability. *Sci. Adv.* **2**, e1600225 (2016).
- [17] D. S. De, B. Schaefer, B. von Issendorff, and S. Goedecker, Nonexistence of the decahedral $\text{Si}_{20}\text{H}_{20}$ cage: Levinthal’s paradox revisited, *Phys. Rev. B* **101**, 214303 (2020).
- [18] P. Giannozzi *et al.*, Advanced capabilities for materials modelling with Quantum ESPRESSO, *J. Phys.: Condens. Matter* **29**, 465901 (2017).
- [19] J. P. Perdew, K. Burke, and M. Ernzerhof, Generalized Gradient Approximation Made Simple, *Phys. Rev. Lett.* **77**, 3865 (1996).
- [20] A. Dal Corso, Pseudopotentials periodic table: From H to Pu, *Computational Material Science* **95**, 337 (2014).
- [21] H. J. Monkhorst and J. D. Pack, Special points for Brillouin-zone integrations, *Phys. Rev. B* **13**, 5188 (1976).
- [22] N. Marzari, D. Vanderbilt, A. De Vita, and M. C. Payne, Thermal Contraction and Disordering of the Al(110) Surface, *Phys. Rev. Lett.* **82**, 3296 (1999).
- [23] S. Baroni, S. Gironcoli, A. D. Corso, and P. Giannozzi, Phonons and related crystal properties from density-functional perturbation theory, *Rev. Mod. Phys.* **73**, 515 (2001).
- [24] Y. Zhang, G. Kresse, and C. Wolverton, Nonlocal First-Principles Calculations in Cu-Au and Other Intermetallic Alloys, *Phys. Rev. Lett.* **112**, 075502 (2014).
- [25] A. Jain, S. P. Ong, G. Hautier, W. Chen, W. D. Richards, S. Dacek, S. Cholia, D. Gunter, D. Skinner, G. Ceder, K. A. Persson, The Materials Project: A materials genome approach to accelerating materials innovation, *APL Materials*, **1**, 011002 (2013).
- [26] S. P. Ong, W. D. Richards, A. Jain, G. Hautier, M. Kocher, S. Cholia, D. Gunter, V. L. Chevrier, K. A. Persson, and G. Ceder, Python Materials Genomics (pymatgen): A robust, open-source python library for materials analysis, *Comput. Mater. Sci.* **68**, 314 (2013).
- [27] See Supplemental Materials at XXX, which includes the phonon dispersion curves of 40 binary alloys, listed in Table I, in the bHC structure, those of AlSn alloys in the B_h and bHC structures, and those of AlCu in the bHC structure.
- [28] J. P. Perdew, A. Ruzsinszky, G. I. Csonka, O. A. Vydrov, G. E. Scuseria, L. A. Constantin, X. Zhou, and K. Burke, Restoring the Density-Gradient Expansion for Exchange in Solids and Surfaces, *Phys. Rev. Lett.* **100**, 136406 (2008).
- [29] J. Yuhara, M. Schmid, and P. Varga, Two-dimensional alloy of immiscible metals: Single and binary monolayer films of Pb and Sn on Rh(111), *Phys. Rev. B* **67**, 195407 (2003).
- [30] J. Yuhara, M. Yokoyama, T. Matsui, A two-dimensional alloy of immiscible Bi and Sn atoms on Rh(111), *Surf. Sci.* **606**, 456 (2012).
- [31] S. Haastруп, M. Strange, M. Pandey, T. Deilmann, P. S. Schmidt, N. F. Hinsche, M. N. Gjerding, D. Torelli, P. M. Larsen, A. C. Riis-Jensen, J. Gath, K. W. Jacobsen, J. J. Mortensen, T. Olsen, and K. S. Thygesen, The Computational 2D Materials Database: high-throughput modeling and discovery of atomically thin crystals, *2D Materials* **5**, 042002 (2018).